BIOCHEMISTRY
including biophysical chemistry & molecular biology

Article

pubs.acs.org/biochemistry

Insights into the Role of Asp79$^{2.50}$ in β_2 Adrenergic Receptor Activation from Molecular Dynamics Simulations

Anirudh Ranganathan,[†,‡] Ron O. Dror,[§] and Jens Carlsson*[,†,‡]

[†]Science for Life Laboratory, Box 1031, SE-171 21 Solna, Sweden

[‡]Department of Biochemistry and Biophysics and Center for Biomembrane Research, Stockholm University, SE-106 91 Stockholm, Sweden

[§]Department of Computer Science, Department of Molecular and Cellular Physiology, and Institute for Computational and Mathematical Engineering, Stanford University, Stanford, California 94305, United States

Supporting Information

ABSTRACT: Achieving a molecular-level understanding of G-protein-coupled receptor (GPCR) activation has been a long-standing goal in biology and could be important for the development of novel drugs. Recent breakthroughs in structural biology have led to the determination of high-resolution crystal structures for the β_2 adrenergic receptor (β_2AR) in inactive and active states, which provided an unprecedented opportunity to understand receptor signaling at the atomic level. We used molecular dynamics (MD) simulations to explore the potential roles of ionizable residues in β_2AR activation. One such residue is the strongly conserved Asp79$^{2.50}$, which is buried in a transmembrane cavity and becomes dehydrated upon β_2AR activation. MD free energy calculations based on β_2AR crystal structures suggested an increase in the population of the protonated state of Asp79$^{2.50}$ upon activation, which may contribute to the experimentally observed pH-dependent activation of this receptor. Analysis of MD simulations (in total >100 μs) with two different protonation states further supported the conclusion that the protonated Asp79$^{2.50}$ shifts the conformation of the β_2AR toward more active-like states. On the basis of our calculations and analysis of other GPCR crystal structures, we suggest that the protonation state of Asp$^{2.50}$ may act as a functionally important microswitch in the activation of the β_2AR and other class A receptors.

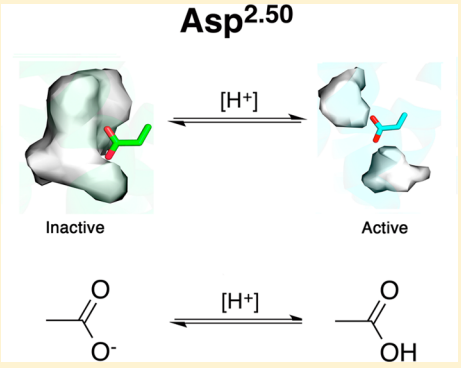

The G-protein-coupled receptors (GPCRs) make up a large family of membrane-bound proteins[1] that have received considerable attention in drug discovery. GPCRs signal across cellular membranes in response to the presence of hormones, neurotransmitters, and a wide variety of other extracellular molecules. In particular, the binding of certain ligands to the extracellular (orthosteric) binding site of a GPCR favors a conformational change in the receptor known as activation, which facilitates coupling of the receptor to cytosolic G-proteins. Drugs may act by favoring activation (agonists), disfavoring it (inverse agonists), or simply blocking the binding of other ligands to the orthosteric site (neutral antagonists).

A long-standing goal of GPCR research is to understand the mechanism of activation in atomistic detail. A major step toward this goal has been the determination of multiple high-resolution structures for GPCRs,[2] which provided invaluable insights into how signaling across the cell membrane is accomplished. One of the prototypical GPCRs is the β_2 adrenergic receptor (β_2AR). There are now crystal structures of the β_2AR in both the inactive state,[3] with a bound inverse agonist, and the active state complex with an agonist and G-protein.[4] These structures demonstrated that activation involves only subtle changes in the orthosteric site, which shifts the conformational equilibrium on the cytosolic side toward an active state characterized by a ∼14 Å shift for transmembrane (TM) helix 6 and G-protein binding.[4,5] Interestingly, the reorganization of the transmembrane helices for the β_2AR were remarkably similar to those present in the crystal structures of opsin,[6,7] the A_{2A} adenosine receptor[8,9] (A_{2A}AR), and the M_2 muscarinic receptor (M_2MR)[10,11] in active-like states, which suggested that GPCRs share features in their activation mechanism.[2] However, crystal structures provide only static pictures of GPCR signaling, and it is still not entirely clear how the signal induced by agonist binding is transmitted to the intracellular side. It is evident that the conformational ensemble available to the β_2AR cannot simply be divided into active and inactive states.[12] NMR and fluorescence spectroscopy experiments have instead supported a diverse energy landscape, which leads to different conformational ensembles of the receptor depending on the nature of the bound ligand and the presence of intracellular binding partners.[13−16] Both crystal structures and molecular dynamics (MD) simulations of the β_2AR have suggested an allosteric network connecting the orthosteric site and the intracellular

Received: July 15, 2014
Revised: October 21, 2014
Published: October 27, 2014

domain,[17−21] but it is still not clear how more receptor specific signaling properties, such as activation of different intracellular pathways or basal activity, are encoded in the three-dimensional structures.

Biophysical and biochemical experiments have identified conserved sequence motifs that appeared to be key components of the activation mechanism.[22−24] As crystal structures of GPCRs in inactive and active states are now available, the role of these "molecular switches" can be analyzed at the atomic level. One such proposed switch is a salt bridge between the strongly conserved Arg$^{3.50}$ in the "DRY motif" and Glu$^{6.30}$ in TM helix 6 (superscripts represent Ballesteros−Weinstein numbering[25]), which was proposed to stabilize the inactive state and become disrupted upon activation (termed the "ionic lock").[23] The ionic lock has been absent in inactive state β_2AR crystal structures but was demonstrated to form in MD simulations[18,20] and was subsequently observed in structures of the closely related β_1AR.[26] As expected, the ionic lock was found to be broken in active conformations of the β_2AR.[4] Similarly, the rotameric state of conserved residue Trp$^{6.48}$ has been hypothesized to act as a "toggle switch" that modulates the equilibrium between the active and inactive conformations of TM helix 6.[23,24] Considerable focus is now being directed toward understanding how GPCRs are allosterically regulated, e.g., by cholesterol, water molecules, or ions.[2,27−29] Crystal structures of the β_2AR and A_{2A}AR have revealed specific binding sites for cholesterol.[27] Recent high-resolution structures of class A GPCRs [A_{2A}AR,[28,30] δ-opioid receptor (δ-OR),[28] protease-activated receptor 1 (PAR1),[31] and thermostabilized β_1AR[32]] also led to the identification of an ion binding site in the transmembrane region, which explained the sodium-dependent effects on activation observed for several of these receptors.[28] Clusters of water molecules in the transmembrane region are also conserved across multiple crystal structures, and many of these interact with conserved residues, suggesting that they may be involved in receptor activation.[33−35] GPCR activation and ligand binding have also been shown to be pH-dependent in several cases, which suggests that ionizable residues may be important for receptor function.[36−38] However, the resolution of GPCR crystal structures does not typically allow identification of water networks and protonation states of ionizable residues, which makes it difficult to understand the potential roles of these in signaling.

The focus of this work was to investigate the pH dependence of activation for the β_2AR and, more generally, the role of conserved ionizable residue Asp$^{2.50}$ in GPCR signaling. Kobilka and co-workers have shown that both basal activity and the level of agonist-induced activation for the β_2AR are greater at pH 6.5 than at pH 8,[37] which suggested that changes in the protonation states of ionizable residues are involved in activation. As expected, a majority of the ionizable residues were found to be solvent-exposed and not likely to be involved in the observed pH dependence. Five acidic residues (Asp$^{2.50}$, Asp$^{3.32}$, Glu$^{3.41}$, Asp$^{3.49}$, and Glu$^{6.30}$) were identified as candidates for the pH dependence of activation, and three of these were mutated to alanine (Glu$^{3.41}$, Asp$^{3.49}$, and Glu$^{6.30}$). Among these were Asp$^{3.49}$, which has been shown to be responsible for the pH-dependent activation of rhodopsin,[38] and Glu$^{6.30}$, which has been suggested to be important for stabilizing the inactive state by engaging in an "ionic lock" with Arg$^{3.50}$. None of the three investigated mutants significantly altered the pH dependence of basal activity observed for the wild-type receptor. This suggested that the pH dependence of activation for the β_2AR, in contrast to that for rhodopsin, cannot be explained solely by the protonation of Asp$^{3.49}$ but that other ionizable residues must also play a role. The potential roles of residues Asp$^{2.50}$ and Asp$^{3.32}$ were not investigated in the study by Kobilka and co-workers because mutations at these positions resulted in nonfunctional receptors. Asp$^{3.32}$ is conserved among the aminergic GPCRs and is directly involved in agonist and antagonist binding. Asp$^{2.50}$ is conserved in 94% of all class A GPCRs[39] and is part of a buried cavity in the transmembrane region. While Asp$^{2.50}$ is not directly involved in orthosteric ligand binding, it has been shown to be critical for signaling in mutagenesis studies and suggested to be involved in the conformational changes associated with activation.[40−44]

Identification of the residue(s) responsible for the pH-dependent behavior of the β_2AR could provide insights into how this receptor is modulated by protons and shed further light on the mechanism of activation. To investigate the pH dependence of β_2AR activation, we conducted a series of MD free energy calculations focused on determining the change in pK_a values for Asp$^{2.50}$ and Asp$^{3.32}$ upon activation. The free energy calculations predicted a large increase in pK_a for Asp$^{2.50}$, which provided an explanation for the increase in β_2AR basal activity and activation at low pH values. Analysis of more than 100 μs of MD simulations with ionized and protonated Asp$^{2.50}$ supported the possibility that the ionization state of this residue might affect the equilibrium between active and inactive conformations in the TM region. Together, our results suggest that protonation of Asp$^{2.50}$ could be one of the important microswitches in activation of the β_2AR and other class A GPCRs.

METHODS

Molecular Dynamics Free Energy Calculations. The MD free energy calculations were performed using crystal structures for the inactive [Protein Data Bank (PDB) entry 2RH1[3]] and active states (PDB entry 3SN6[4]) of the β_2AR. In the first step, a hydrated POPC membrane was first equilibrated around the β_2AR structure using periodic boundary conditions in GROMACS4.5[45] with the OPLSAA force field,[46] TIP3P waters,[47] and Berger lipids.[48] In this simulation, all protein atoms were tightly restrained to their initial coordinates and the hydrated membrane was equilibrated for 40 ns at 300 K. The free energy calculations were conducted starting from the membrane-equilibrated β_2AR systems using spherical boundary conditions in the program Q.[49] The same force field parameters for protein, water, and lipids were used, and parameters for the ligands were obtained using Schrodinger's program hetgrp_ffgen [part of Schrodinger utilities software (http://www.schrodinger.com)]. The simulations were conducted at a constant temperature of 310 K[49,50] in a spherical droplet with a radius of of 26 Å centered on the Cγ atom of Asp$^{2.50}$ or Asp$^{3.32}$. All atoms within 26 Å of the center of the sphere were explicitly included in the simulations. Atoms outside the sphere were tightly restrained to their initial coordinates and excluded from nonbonded interactions. Asp, Glu, His, Lys, and Arg residues within the spherical system were assigned protonation states by manual inspection. Apart from Asp$^{2.50}$ and Asp$^{3.32}$, the only ionizable residue in the transmembrane region is Glu122, which was kept neutral in all simulations. The total charge of the sphere was zero in all cases, which was accomplished by either adjusting charges of ionzable

dx.doi.org/10.1021/bi5008723 | Biochemistry 2014, 53, 7283−7296

residues at the sphere edge or adding sodium ions to the system. This was done to avoid problems associated with insufficient solvent shielding of surface charges and to eliminate contributions from the Born term that arises when the carboxylate becomes charged in the free energy calculations.[51] The SHAKE algorithm[52] was applied to all solvent bonds and angles, and the water molecules at the sphere surface were subjected to radial and polarization restraints.[49,53] A nonbonded cutoff of 10 Å was used for all atoms except for the atoms that change force field parameters in the FEP calculation, for which no cutoff was applied. Long-range electrostatic interactions were treated with the local reaction field (LRF) multipole expansion method.[54] The time step was set to 1 fs, and nonbonded pair lists were updated every 25 steps.

To compute the relative free energy of deprotonation, the aspartic acid of interest (Asp113$^{3.32}$ or Asp79$^{2.50}$) was alchemically transformed from protonated to ionized in inactive and active conformations of the β_2AR.[55] The free energy of deprotonation was computed using the free energy perturbation (FEP) technique, and the calculation was conducted via several intermediates. The potentials governing the intermediate states are defined by $U_m = \lambda_m U_A + (1 - \lambda_m)U_B$, where A and B represent two different end states, in this case the ionized and protonated aspartic acid residue, respectively, and λ_m is a mapping parameter that varies from 0 to 1. The free energy difference between states A and B can be calculated by summing up the free energy differences of the n intermediate states using

$$\Delta G^{\mathrm{FEP}}_{\mathrm{A}\rightarrow\mathrm{B}} = -kT \sum_{m=1}^{n-1} \ln\langle e^{-(U_{m+1}-U_m)/kT}\rangle_m$$

where $\langle ... \rangle_m$ represents an ensemble average on the potential U_m, which is calculated from MD simulations.[55] The free energy was computed in 22 steps, in which the partial charges, van der Waals parameters, and torsional parameters were changed according to the OPLSAA force field. At each of the 23 λ states (1, 0.95, 0.9, 0.85, 0.8, 0.75, 0.7, 0.65, 0.6, 0.55, 0.5, 0.45, 0.4, 0.35, 0.3, 0.25, 0.2, 0.15, 0.1, 0.06, 0.04, 0.02, and 0), an equilibration, in which harmonic restraints on the solute atoms were gradually released, was performed for 0.7 ns. The equilibration was followed by unrestrained simulation for 1.5 ns for each λ value, in which energies were extracted every 50 fs. Three independent simulations were conducted for each λ state, and the energies were combined to calculate the free energy (simulations A–C, F, and G in Table S1 of the Supporting Information) The errors were estimated from the difference between the forward and backward summation of free energies. In theory, the contributions from distant charges (at the sphere border and outside the sphere) must be added, for example, using a screened Coulombic potential.[56] However, as the difference in free energy between the active and inactive state structures was taken, this term was essentially negligible. The relative pK_a difference for the residue of interest (Asp113$^{3.32}$ or Asp79$^{2.50}$) between the active and inactive states of the receptor is calculated as the difference in the free energy of deprotonation divided by $RT \ln(10)$ = 1.4 kcal/mol.

PROPKA Calculations. The empirical pK_a calculations were performed using PROPKA3.0 and PROPKA3.1.[57] All parts of the structure that were not part of the receptor or associated G-protein in the case of active structures were removed. In all cases, the pK_a values were determined in the absence of a membrane. The absence of phospholipids should not affect the calculations significantly as this method estimates the pK_a value from local interactions and the considered aspartic acid residues are buried in the core of the receptor. Five crystal structures were used to predict the pK_a of Asp79$^{2.50}$ in the inactive state (PDB entries 2RH1, 3NY8, 3NY9, 3NYA, and 3D4S).[3,27,58] Five β_2AR structures were used to represent the active state conformation (PDB entries 3P0G, 4LDL, 4LDE, 4LDO, and 3SN6).[4,17,59] Four structures were used for the rhodopsin/opsin inactive state pK_a calculations (PDB entries 1F88, 3C9L, 1U19, and 1GZM).[60−65] Four structures (PDB entries 3CAP, 3PQR, 3PXO, and 3DQB) were used for the active state pK_a calculations of rhodopsin.[6,7] For the active-like rhodopsin/opsin structures, the positions of atoms OD1 and ND2 of residue Asn55$^{1.50}$ were altered in line with the hydrogen bonding environment around this residue. Nine structures were used for the A_{2A}AR inactive state pK_a calculations (PDB entries 3EML, 3RFM, 3VGA, 3VG9, 3UZA, 3UZC, 4EIY, 3REY, and 3PWH).[8,9,66−68] Three structures of the A_{2A}AR were used for the active-like state pK_a calculations (PDB entries 3QAK, 2YDO, and 2YDV).[8,9]

Molecular Dynamics Simulations of the Inactive State Using Periodic Boundary Conditions. The MD simulations for the β_2AR were performed using a crystal structure of the inactive state of the receptor (PDB entry 2RH1[3]). The T4 lysozyme insertion was removed from the structure, and as in previous studies, intracellular loop 3 was not included in the simulations.[18] The membrane and solvent were first equilibrated as described in the previous section. The dimensions of the equilibrated system roughly measured 94 Å × 94 Å × 105 Å and included 232 lipid molecules and 15946 water molecules. The coordinates from this equilibration were taken as the starting point for two simulations with protonated and ionized Asp79$^{2.50}$. The number of ions in the system was adjusted to maintain the overall neutrality of the system. The temperature was kept constant using a Nose-Hoover thermostat,[69,70] while the pressure was maintained at 1 bar using a semi-isotropic Parrinello-Rahman barostat[71] with a coupling of 2 ps. A compressibility value of 4.5 × 10^{-5} bar^{-1} was used. The long-range interactions were calculated using the particle mesh Ewald (PME) method.[72] A 1.2 nm cutoff was used for short-range interactions. The LINCS algorithm was used to constrain bond lengths in all atoms of the system.[73] The two systems were then equilibrated for 1.25 ns in GROMACS4.5[45] at 310 K using a 2 fs time step. During the equilibration, the harmonic restraints on the protein atoms were gradually released. This was followed by a total of 1.1 and 1.7 μs [two independent simulations of 1.1 and 0.6 ns, respectively (simulations D and E, respectively, in Table S1 of the Supporting Information)] of unrestrained production runs at 310 K with the ionized and protonated Asp79$^{2.50}$, respectively.

Cavity Volume Calculations. Cavity volumes were calculated using the mdpocket suite of the fpocket program.[74] Pocket identification was performed using values slightly lower than the default parameters for mdpocket, with a minimum sphere size of 2.65 Å and a maximum of 5.5 Å. Calculations of cavity volume over all the snapshots were then performed using a minimum sphere size of 2.5 Å and a maximum of 5.5 Å, to obtain a better description of the cavity volume. For the simulations that were conducted in this work, the volume was calculated using 110 snapshots from the 1.1 μs simulation with the ionized Asp79$^{2.50}$ and 170 snapshots for the simulations, totalling 1.7 μs for the protonated Asp79$^{2.50}$. MD simulation trajectories of the β_2AR generated by Dror et al., which were

dx.doi.org/10.1021/bi5008723 | Biochemistry 2014, 53, 7283−7296

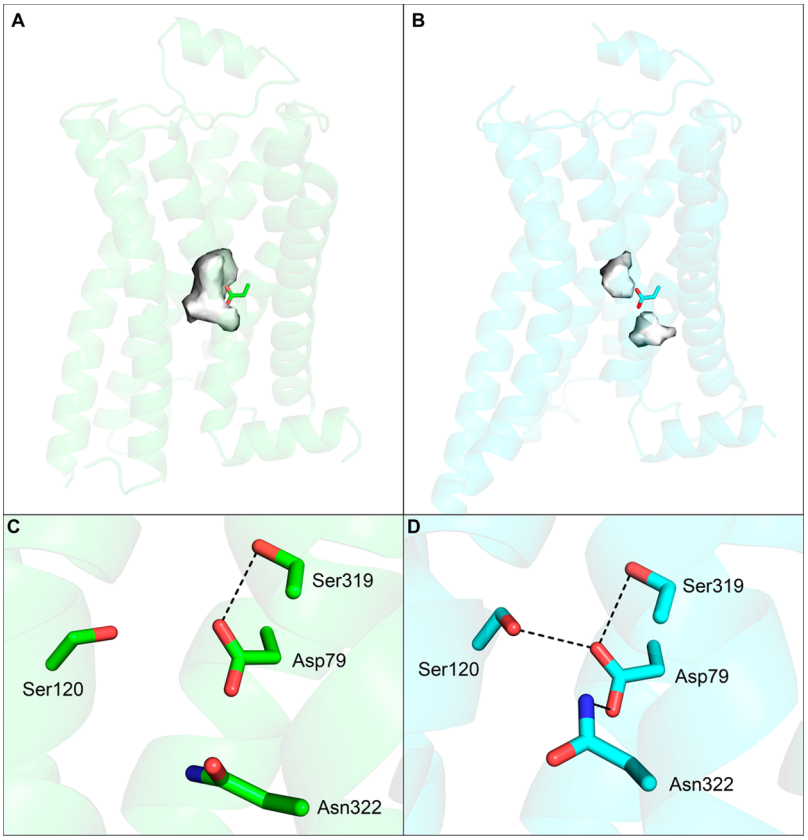

Figure 1. Analysis of conformational changes upon β_2AR activation for Asp79$^{2.50}$ based on crystal structures. Crystal structures of inactive (A and C) and active (B and D) states of the β_2AR (PDB entries 2RH1 and 3SN6, respectively). Hydrogen bonds are shown as black dashed lines. This figure was generated with PyMOL (version 1.4.1).

initiated from an active conformation, were also analyzed.[19] The five simulations with the ionized Asp79$^{2.50}$ (simulation H in Table S1 of the Supporting Information) correspond to condition "D" in the original work (see Table S1 of the Supporting Information of Dror et al.[19]) using the trajectories with lengths of 10.0, 8.0, 6.4, 5.0, and 5.0 μs. The four trajectories with the protonated Asp79$^{2.50}$ (simulation I in Table S1 of the Supporting Information) correspond to condition "I" in the original work.[19] Snapshots were obtained every 18 ns, which resulted in 1867 and 4249 snapshots in total with the ionized and protonated Asp79$^{2.50}$, respectively.

RESULTS

Analysis of Conformational Changes upon β_2AR Activation Based on Crystal Structures. pK_a values of ionizable residues vary by several units depending on the local environment, and their protonation states can strongly influence the conformation of a protein. Thus, at a microscopic level, the pH dependence of protein function is determined by the protonation states of its ionizable residues. The observed pH dependence of β_2AR activation suggested that the protonation state for one or several ionizable residue favors active conformations of the receptor at low pH.[37] In a first step, structural changes upon β_2AR activation that involve ionizable residues were analyzed on the basis of available crystal structures. Particular focus was placed on Asp79$^{2.50}$ and Asp113$^{3.32}$ as these had been suggested to be candidates for involvement in the pH dependence of β_2AR activation, but it was difficult to assess the roles of these experimentally.[37]

Asp79$^{2.50}$ is deeply buried in the transmembrane region and is in close contact with several conserved sequence motifs in class A GPCRs, e.g., the NPxxY motif in TM helix 7. Asp$^{2.50}$ is present in 94% of all class A GPCRs, and such strong conservation of an aspartic acid in the transmembrane region is indicative of a functional role as burial of an ionizable residue is energetically unfavorable.[75] The crystal structures of inactive and active states of the β_2AR revealed that the environment surrounding Asp79$^{2.50}$ changes significantly upon activation. In the inactive state, Asp79$^{2.50}$ is located in a cavity with up to 10−12 water molecules. The volume of this cavity was found to range between 287 and 396 Å^3 with an average of ∼350 Å^3 based on five crystal structures of the β_2AR (Figure 1A and Table S2 of the Supporting Information). The side chain carboxylate of Asp79$^{2.50}$ mainly interacts with cavity waters but also forms a hydrogen bond with Ser319$^{7.46}$. In addition, the residue forms a network of water-mediated contacts to Ser120$^{3.39}$ and Asn322$^{7.49}$ (Figure 1C). In the active state of the β_2AR, a majority of all water molecules are expelled from the Asp79$^{2.50}$ cavity and its volume is reduced to an average of ∼200 Å^3, with values ranging from 170 and 231 Å^3 (Table S2 of the Supporting Information).[4] This contraction involves the tilting of TM helices 3 and 7 with several side chains moving into the cavity. The conformational changes bring strongly conserved residues, e.g., Ser120$^{3.39}$ and Asn322$^{7.49}$, within direct hydrogen bonding distance of the side chain carboxylate of Asp79$^{2.50}$ (Figure 1D). The large structural changes in the vicinity of Asp79$^{2.50}$ upon activation suggested that this residue could be responsible for the observed pH dependence of β_2AR function.

dx.doi.org/10.1021/bi5008723 | *Biochemistry* 2014, 53, 7283−7296

A second residue hypothesized to be responsible for the pH dependence of activation was Asp113$^{3.32}$, which is located in the orthosteric site and involved in both agonist and antagonist binding.[37] The structure of the orthosteric site of the β_2AR was found to be relatively rigid as judged by similar receptor conformations for the receptor in complex with ligands of varying efficacies.[58] The conformational changes in orthosteric site upon activation of the β_2AR essentially only involved slight contraction of the binding pocket.[4,17] The differences in the local environment around Asp113$^{3.32}$ between the active and inactive states were significantly smaller than in the case of Asp79$^{2.50}$. The interactions with the surrounding residues remain the same in both crystal structures (Figure 2), which

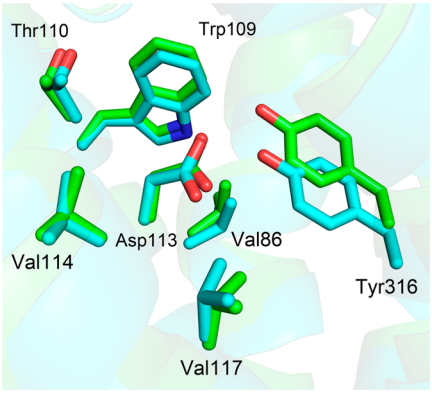

Figure 2. Analysis of conformational changes upon β_2AR activation for Asp113$^{3.32}$ based on crystal structures. Crystal structures of inactive (PDB entry 2RH1, green) and active (PDB entry 3SN6, cyan) states of the β_2AR. This figure was generated with PyMOL (version 1.4.1).

suggested that activation would not result in a significant shift of protonation for this residue. In addition, as both inverse agonists and agonists of the β_2AR typically are cations, Asp113$^{3.32}$ should remain ionized in both active and inactive conformations of the receptor.

Shift in the Protonation State of Asp79$^{2.50}$ upon Activation of the β_2AR from MD Free Energy Calculations. To further quantify changes in protonation for Asp79$^{2.50}$ upon activation, we turned to MD simulations with explicit representation of protein, membrane, and water molecules. In contrast to the static crystal structures, the simulations involve averaging over a large number of conformations and accurately accounts for shifts in protonation caused by changes in receptor structure and desolvation. As absolute pK_a values are challenging to predict accurately with current force fields,[76] the free energy calculations were complemented by empirical methods to assess if changes in protonation states would occur in a pH range relevant for physiological conditions.

Compared to Vanni et al.,[20] we had the advantage of access to crystal structures of both active and inactive states of the β_2AR. The shift in pK_a value upon activation could thus be computed directly from a thermodynamic cycle that involves calculation of the free energy of deprotonation from MD simulations of the crystallographic structures in inactive and active states (Figure S1 of the Supporting Information).[56,76,77] The MD simulations were conducted in a sphere with a radius of 26 Å centered on the aspartic acid residue of interest. Atoms within the sphere were treated as flexible in the simulation, whereas residues outside this radius were tightly restrained to their crystal coordinates to maintain the receptor in the active or inactive conformation. For example, the spherical system involving calculations for Asp79$^{2.50}$ included the cavity surrounding this residue, the orthosteric site, and conserved residues (e.g., the ionic lock and NPxxY motifs), as well as the parts of the G-protein that interact with the receptor in the active state (Figure S2 of the Supporting Information). The pK_a value of Asp79$^{2.50}$ was not expected to be strongly coupled to any other ionizable residues as these were >10 Å away. In the case of Asp79$^{2.50}$, calculations were conducted in the presence and absence of the cocrystallized ligands to investigate the potential influence of ligand binding on the pK_a of this residue. On the basis of the crystal structures, we did not expect a shift in pK_a for Asp113$^{3.32}$, but for comparison, we also calculated the change in free energy of deprotonation for this residue in the absence of orthosteric ligands.

The deprotonation of the side chain carboxylate was conducted in 22 steps in which a negative charge was gradually introduced on the residue. The free energy change for each step was calculated using Zwanzig's formula, and the total free energy of deprotonation was calculated as the sum of all steps.[55] The number and distribution of states were optimized to achieve converged free energies with errors of <1 kcal/mol. As an additional control experiment, the free energy of deprotonation was calculated for the Oδ1 and Oδ2 carboxylate atoms, which yielded very similar pK_a shifts for both Asp79$^{2.50}$ and Asp113$^{3.32}$. In total, more than 100 ns was used to calculate each free energy of deprotonation. No large structural fluctuations were observed within the sphere in these simulations, and the average backbone rmsds from the crystal structure for the Asp79$^{2.50}$ calculations remained <0.5 Å for both the active and inactive conformations throughout the simulation. The changes in free energy as the side chain carboxylate of Asp79$^{2.50}$ was deprotonated in the inactive and active state are shown in Figure S3 of the Supporting Information.

The calculated free energies of deprotonation for Asp79$^{2.50}$ and Asp113$^{3.32}$ in the inactive and active states of the β_2AR are listed in Table 1. The shift in the free energy of deprotonation for Asp79$^{2.50}$ upon activation was 4.5 kcal/mol for the ligand-bound structures and 5.3 kcal/mol for the apo structures. These

Table 1. Summary of Calculated Free Energies of Deprotonation from MD Simulations[a]

		$\Delta G_{deprotonation}$ (kcal/mol)			
residue	orthosteric ligand	inactive	active	$\Delta\Delta G_{deprotonation}$ (kcal/mol)	ΔpK_a
Asp79$^{2.50}$	yes	−48.9 ± 0.2	−44.4 ± 0.1	4.5 ± 0.3	3.2
Asp79$^{2.50}$	no	−49.1 ± 0.2	−43.8 ± 0.2	5.3 ± 0.4	3.7
Asp113$^{3.32}$	no	−59.4 ± 0.4	−58.4 ± 0.1	1.0 ± 0.6	0.7

[a]Free energies of deprotonation for Asp79$^{2.50}$ and Asp113$^{3.32}$ of the β_2AR from MD free energy calculations and the difference in pK_a between inactive and active state conformations.

dx.doi.org/10.1021/bi5008723 | Biochemistry 2014, 53, 7283−7296

differences corresponded to pK_a shifts of 3.2 and 3.7 units, respectively, suggesting that the protonated Asp79$^{2.50}$ was significantly more favored in the active conformation. The pK_a shift was thus due to the receptor conformations, rather than the presence of the orthosteric ligands themselves. For Asp113$^{3.32}$, no large changes in conformation could be identified from the structural analysis of the orthosteric site of the β_2AR crystal structures, and the free energies of deprotonation were also significantly smaller [0.7 pK_a unit (Table 1)] compared to that of Asp79$^{2.50}$. This small shift was likely due to the slight contraction of the orthosteric site observed upon activation.[17]

To understand the large shift in pK_a upon activation obtained in the free energy calculations for Asp79$^{2.50}$, we analyzed the interaction energies between Asp79$^{2.50}$ and the receptor and solvent separately. As expected for ionization free energies, a majority of the contribution to the pK_a shift was due to changes in electrostatic interactions. To investigate the balance between solvent and protein contributions to the free energy, the electrostatic interaction energies between Asp79$^{2.50}$ and its surroundings were calculated for the protonated and ionized side chain carboxylate, which is summarized in Figure 3. The

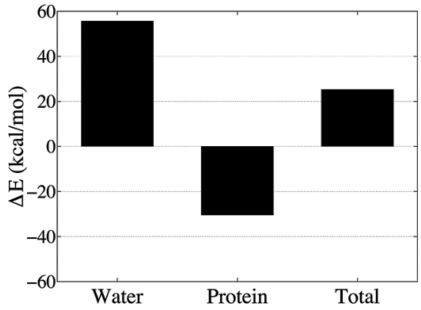

Figure 3. Energetic contributions from water and protein to the Asp79$^{2.50}$ pK_a shift. Change in electrostatic interaction energies (ΔE) between the protonated and ionized Asp79$^{2.50}$ upon activation from the MD free energy calculations. The electrostatic interactions with protein and water and the total are shown separately.

electrostatic interaction energies with water for the protonated Asp79$^{2.50}$ were similar in both the active and inactive states (−13.8 and −12.3 kcal/mol, respectively), whereas they were significantly more favored in the inactive state for the ionized Asp79$^{2.50}$ (−79.7 kcal/mol) than in the active state (−25.5 kcal/mol). This 54.2 kcal/mol difference in interaction energy was compensated by favorable electrostatics of −33.4 kcal/mol with the protein in the active state, but the net result was a large stabilization of the ionized Asp79$^{2.50}$ in the inactive state. This agreed well with the inactive and active state β_2AR crystal structures. Activation involves a contraction of the cavity around Asp79$^{2.50}$, leading to a reduction in the number of solvent interactions for the side chain carboxylate. This loss of favorable electrostatic interactions leads to a strong stabilization of the protonated form of Asp79$^{2.50}$ in the active state. Two representative MD simulation snapshots of the ionized Asp79$^{2.50}$ in the active and inactive states are shown in Figure 4.

Whereas the free energy calculations showed that the pK_a of Asp79$^{2.50}$ was shifted toward higher values in the active state, it was not clear if shifts in protonation would occur in a pH range relevant for physiological conditions. An estimate of the absolute pK_a values of Asp79$^{2.50}$ was obtained using the PROPKA method,[57] which is a widely used empirical approach to investigate the protonation states of ionizable residues in proteins. In a recent benchmark of empirical and continuum electrostatics approaches, PROPKA was found to be the most accurate method for the prediction of absolute pK_a values.[78] As the PROPKA method is orders of magnitude faster than MD free energy calculations, a large number of β_2AR crystal structures could be included in these calculations. We did not attempt to quantify the shift in pK_a upon activation as the method is based on static structures and empirical methods generally have problems with predictions of desolvation penalties, which were found to be the main source of the shift in protonation state in the MD free energy calculations.[57,79] Ten high-resolution structures of the β_2AR in the inactive[4,17] or active conformations[4,17,59] were used in the PROPKA calculations. For the inactive β_2AR crystal structures, the pK_a value for Asp79$^{2.50}$ was predicted to be between 6.9 and 8.2. The calculated values for the structures in an active conformation ranged between 7.3 and 8.1. PROPKA thus predicted that the pK_a value of Asp79$^{2.50}$ was elevated to a range relevant under physiological pH conditions (Table S2 of the Supporting Information).

Microsecond Molecular Dynamics Simulations of the β_2AR with Ionized and Protonated Forms of Asp79$^{2.50}$. To investigate how the overall structure of the β_2AR was affected by the protonation state of Asp79$^{2.50}$, we analyzed a set of MD simulations conducted with either ionized or protonated

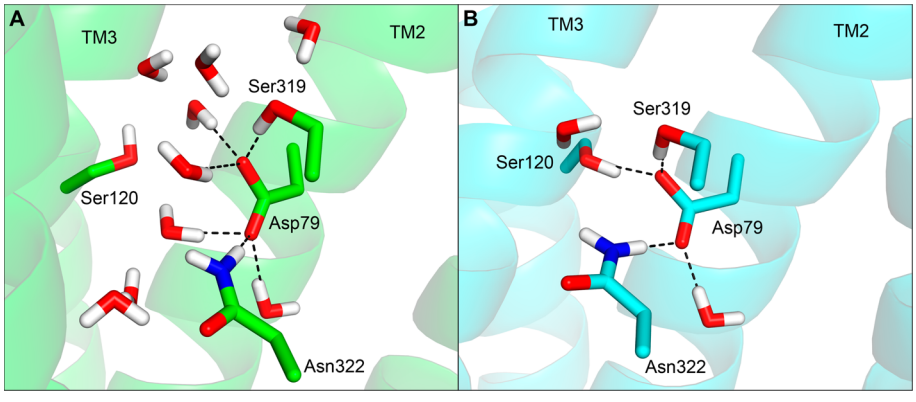

Figure 4. Snapshot from molecular dynamics of ionized Asp79$^{2.50}$ in the inactive and active conformations. Representative snapshot of (A) inactive and (B) active states of the β_2AR. Asp79$^{2.50}$ is ionized, and hydrogen bonds are shown as black dashed lines. This figure was generated with PyMOL (version 1.4.1).

dx.doi.org/10.1021/bi5008723 | *Biochemistry* 2014, 53, 7283−7296

side chain carboxylate. Whereas the free energy calculations were conducted using spherical boundary conditions, which maintained the receptor in an overall active or inactive state, these simulations were conducted with a fully flexible receptor in a hydrated lipid bilayer (Figure S2 of the Supporting Information). First, we conducted simulations initiated from a crystal structure representative of the inactive state of the β_2AR with either protonated or ionized Asp79$^{2.50}$. In a second step, we analyzed a set of previously published MD simulations initiated from an active state crystal structure of the β_2AR, which also were conducted for both protonation states of Asp79$^{2.50}$.[19]

Two sets of MD simulations were first conducted starting from an inactive structure (PDB entry 2RH1[3]). These were performed in the absence of the cocrystallized ligand with two different ionization states of Asp79$^{2.50}$ to investigate the effect of pH on receptor structure. A total of 1.1 and 1.7 μs were generated for the ionized and protonated forms of Asp79$^{2.50}$, respectively (simulations D and E in Table S1 of the Supporting Information). As judged by the rmsd from the backbone atoms to the crystal structure (Figure S4 of the Supporting Information), no large conformational changes were observed in this simulation time, and thus, the receptor remained in conformations representative of the inactive state. One of the major differences between the active and inactive crystal structures was the change in the volume of the hydrated cavity surrounding Asp79$^{2.50}$ (Figure 1). To investigate how the protonation state of Asp79$^{2.50}$ affected the cavity volume, we analyzed both simulation trajectories using the mdpocket program.[74] The cavity volume for the simulation conducted with the ionized Asp79$^{2.50}$ (386 Å^3) was on average larger than in the simulation with the protonated form (304 Å^3). The difference in volume appeared to originate from multiple small changes in the cavity structure, e.g., side chain reorientations for Ser120$^{3.39}$ and Phe282$^{6.44}$. For example, the distance between the Asp79$^{2.50}$ carboxylate oxygen and the side chain oxygen of Ser120$^{3.39}$ was <4 Å in 28% of the snapshots from the simulations with protonated Asp79$^{2.50}$, whereas the occupancy was only 6% in the simulations with the ionized Asp79$^{2.50}$ (Figure S5 of the Supporting Information).

In a second step, we analyzed simulation trajectories that had been initiated from an active state crystal structure of the β_2AR (PDB entry 3P0G[17]). This structure was determined in the presence of a G-protein-mimicking nanobody, which stabilized an active state conformation. Dror et al. conducted simulations of the receptor in complex with the agonist, but without the nanobody.[19] Of the 76 simulation trajectories generated by Dror et al., 39 were found to reach an inactive-like state and were used to elucidate the activation mechanism. These simulations provided an excellent complement to our pK_a calculations as they had been performed with both ionization states for Asp79$^{2.50}$. As our goal was to assess the impact of the Asp79$^{2.50}$ protonation state on β_2AR structure, trajectories were considered irrespective of whether the inactive state was reached in the simulations. Four simulation trajectories with protonated Asp79$^{2.50}$ (a total of 77 μs) and five simulations with ionized Asp79$^{2.50}$ (a total of 34 μs) were analyzed (simulations H and I in Table S3 of the Supporting Information). Two of the analyzed trajectories with each protonation state reached an inactive state, as defined by Dror et al.[19] Each trajectory was first analyzed individually, focusing in particular on changes in the volume of the cavity surrounding Asp79$^{2.50}$. In the simulations with ionized Asp79$^{2.50}$, the cavity quickly grew to a size close to that observed in crystal structures representative of the inactive state in all five simulations (Figure S6 of the Supporting Information). After this initial fast adjustment, the cavity size essentially remained at this larger size in each of these simulations, even when other parts of the receptor underwent substantial conformational changes. In all simulations with protonated Asp79$^{2.50}$, the cavity volume typically remained smaller, close to that representative of the active state (Figure S7 of the Supporting Information), and the cavity size did not appear to depend on the conformational state of the receptor as a whole. As shown in Figure 5, the

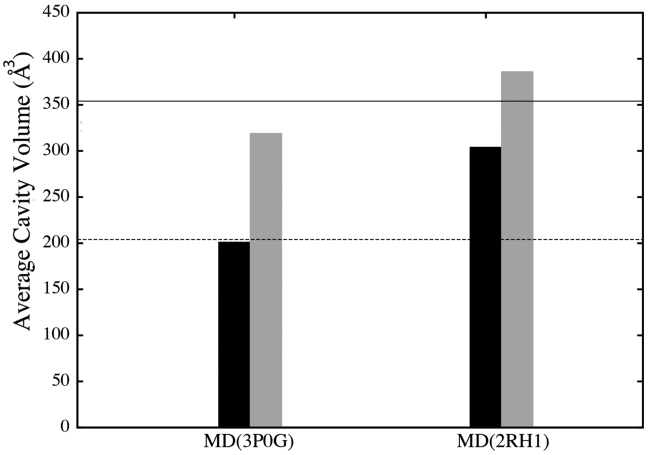

Figure 5. Analysis of molecular dynamics simulations of the β_2AR with ionized and protonated forms of Asp79$^{2.50}$. Average volumes of the cavity surrounding Asp79$^{2.50}$ from MD simulation trajectories and crystal structures. Simulations were conducted with either protonated (black bars) or ionized (gray bars) Asp79$^{2.50}$. Simulations were initiated from both the active (3P0G) and inactive state crystal structures (2RH1). The volumes corresponding to the active and inactive state crystal structures are shown as dashed and solid lines, respectively (Table S2 of the Supporting Information).

average cavity volume was thus significantly larger for the simulations with the ionized Asp79$^{2.50}$ (319 Å^3) compared to simulations with the protonated form (201 Å^3). Two snapshots from the MD simulations that illustrate the difference in cavity volume are shown in Figure 6. Overall, the simulations with ionized Asp79$^{2.50}$ were more consistent with the volumes calculated for the inactive crystal structures, whereas those calculated for trajectories with protonated Asp79$^{2.50}$ were close to that of the active state crystal structures.

The simulations initiated from the active structure of the β_2AR (simulations H and I in Table S1 of the Supporting Information) were analyzed in more detail to further investigate the potential roles of Asp79$^{2.50}$ in activation. Asp$^{2.50}$ has been found to interact with a sodium ion in high-resolution crystal structures of the A_{2A}AR, PAR1, and δ-OR in the inactive state, which explained the negative allosteric effects on agonist binding and activation for many GPCRs.[80] No sodium ion has been observed in the Asp79$^{2.50}$ cavity of the β_2AR, and in contrast to two of the aforementioned GPCRs, it has been demonstrated experimentally that high-affinity agonist binding and basal activity are not affected by sodium chloride.[81] However, considering the strong sequence conservation in the Asp$^{2.50}$ cavity and the fact that a sodium ion was recently observed in a crystal structure of the β_1AR,[32] sodium may also bind to the same site in the β_2AR. Analysis of the five MD

dx.doi.org/10.1021/bi5008723 | Biochemistry 2014, 53, 7283−7296

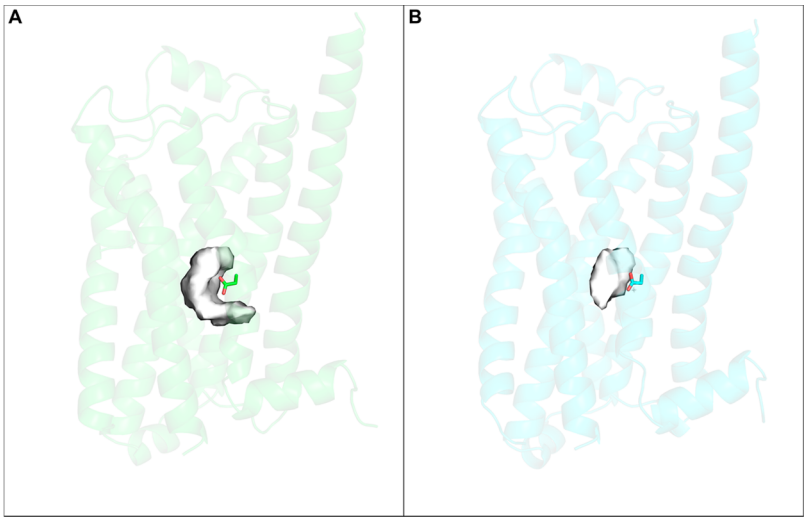

Figure 6. Snapshots from molecular dynamics simulations with protonated and ionized Asp79$^{2.50}$. Snapshots from simulations of the β_2AR with ionized Asp79$^{2.50}$ (A) and protonated Asp79$^{2.50}$ (B), both from simulations initiated from the active conformation of the receptor (PDB entry 3P0G). The cavity is shown as a white surface. This figure was generated with PyMOL (version 1.4.1).

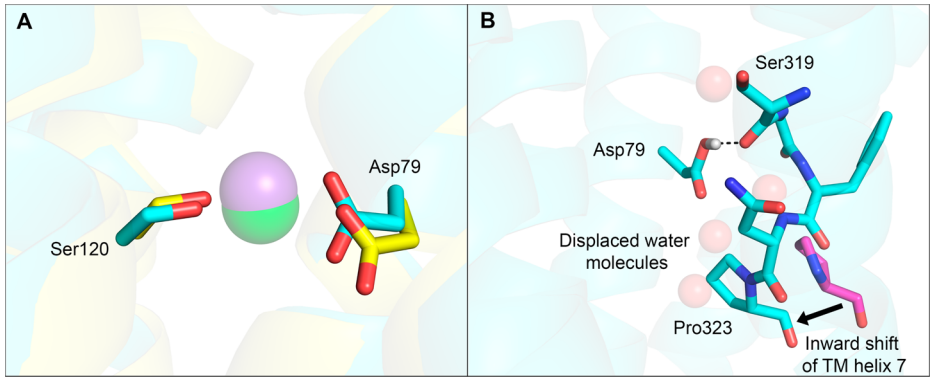

Figure 7. (A) Interactions between a sodium ion and Asp79$^{2.50}$ in a simulation with ionized side chain carboxylate. The carbon atoms of the simulation snapshot are colored cyan, and the sodium ion is depicted as a green sphere. For comparison, the crystal structure of the β_1AR (yellow carbons) with a bound sodium ion (purple sphere) is also shown.[32] (B) The hydrogen bond between protonated Asp79$^{2.50}$ and Ser319$^{7.46}$ stabilizes the inward shift of TM helix 7 relative to the inactive state. The carbon atoms of the simulation snapshot are colored cyan, while those of residue Pro323$^{7.50}$ from the inactive cystal structure (PDB entry 2RH1) are colored purple to illustrate the inward shift of TM helix 7. Water molecules from the inactive state crystal structure that are displaced by the inward shift of TM helix 7 are depicted as transparent red spheres. Hydrogen bonds are shown as black dashed lines. This figure was generated with PyMOL (version 1.4.1).

trajectories with ionized Asp79$^{2.50}$ revealed that a sodium ion entered the expanded (inactive-like) cavity in one trajectory after ~5 μs and remained there throughout the remainder of the simulation. The position of the sodium ion in the Asp$^{2.50}$ cavity also agreed remarkably well with the structure of the β_1AR (Figure 7A). The presence of a sodium ion in the cavity of the β_2ARs would of course only further reduce the pK_a of Asp79$^{2.50}$ in inactive conformations and increase the difference in the level of protonation between active and inactive states. As expected, no sodium ions were observed in the vicinity of Asp79$^{2.50}$ in the simulations with a neutral side chain carboxylate, and the volume of the cavity was significantly smaller compared to those of the corresponding simulations with the ionized residue.

In simulations with a neutral side chain carboxylate, the region surrounding the protonated Asp79$^{2.50}$ adopted several different conformations, including some distinct from those observed in either active or inactive crystal structures.[14,19] In particular, the intracellular end of TM helix 7 sometimes adopted an undistorted α-helical conformation (as in inactive state crystal structures) while shifted inward (as in active state crystal structures) in the vicinity of Asp79$^{2.50}$ (Figure 7B). (This conformation was also noted previously by Dror et al.[19] and Nygaard et al.,[14] who referred to it as the "alternative inactive conformation" or as a conformation on the "alternative deactivation pathway".) This conformation of TM7 was observed only in simulations with Asp79$^{2.50}$ protonated[19] and thus appeared to be stabilized by protonation of this residue. Analysis of interactions in this region revealed that the observed TM helix 7 conformation was stabilized by a hydrogen bond between the carboxylate group and the backbone carbonyl oxygen of Ser319$^{7.46}$, suggesting that the protonation state of Asp79$^{2.50}$ played a key role in maintaining this structure. The formation of this hydrogen bond was strongly correlated with movement of Pro323$^{7.50}$ into a cavity volume occupied by several water molecules in the inactive state crystal structure of the β_2AR (Figure 7B). Interestingly, this inward shift of the strongly conserved residue Pro323$^{7.50}$ and the hydrogen bond interaction between Asp79$^{2.50}$ and TM helix 7 have also been

dx.doi.org/10.1021/bi5008723 | *Biochemistry* 2014, 53, 7283−7296

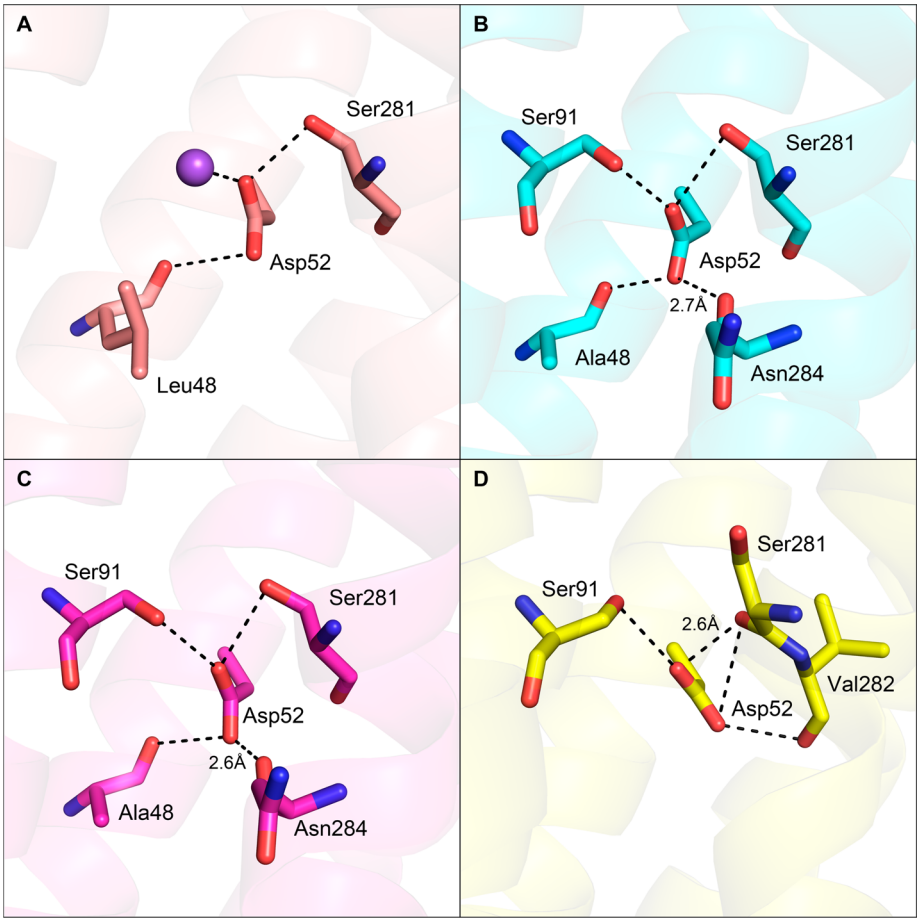

Figure 8. Analysis of the protonation state of Asp$^{2.50}$ in inactive- and active-like crystal structures of the A_{2A}AR: (A) inactive state (PDB entry 4IEY), (B) active-like state (PDB entry 2YDV), (C) active-like state (PDB entry 2YDO), and (D) active-like state (PDB entry 3QAK). Polar contacts within 3.2 Å of the carboxylate oxygens are shown as black dashed lines. The heavy atom distance (Å) is shown if the hydrogen bond is predicted to involve a protonated Asp$^{2.50}$ carboxylate. This figure was generated with PyMOL (version 1.4.1).

observed in an active-like structure of the A_{2A}AR, a point to which we will return.

Analysis of Asp$^{2.50}$ in Other Inactive- and Active-like Crystal Structures of Class A GPCRs. To further investigate the protonation state of Asp$^{2.50}$ in other class A GPCRs, structures of other receptors that had been crystallized in both inactive- and active-like conformations were analyzed. Active- and inactive-like structures were available for the A_{2A}AR, rhodopsin/opsin, and M_2MR. As the M_2MR and β_2AR structures were very similar, we focused on the interactions of Asp$^{2.50}$ for the A_{2A}AR and rhodopsin/opsin.

For the antagonist-bound structures of the A_{2A}AR, a water-filled cavity similar to that in the inactive state of the β_2AR was observed.[67,68,82] In these structures, the side chain carboxylate of Asp52$^{2.50}$ typically formed hydrogen bonds with Ser281$^{7.46}$ and up to four waters in the cavity.[68] The inactive-like A_{2A}AR structure at 1.8 Å resolution revealed that a sodium ion was present in the Asp52$^{2.50}$ cavity, which explained the effects of sodium on agonist binding.[28,30] As the A_{2A}AR cavity is stabilized in the inactive conformation by a bound sodium, Asp52$^{2.50}$ must be ionized in this state to counterbalance the positive charge on the ion (Figure 8A). As observed for the β_2AR, the cavity size was significantly reduced in the three available active-like structures of the A_{2A}AR. Two of the active-like structures were determined for a receptor that had been thermostabilized via four mutations (PDB entries 2YDO and 2YDV[9]), and the third one had been modified by replacing the third intracellular loop with T4-lysozyme.[8] These alterations or the conditions under which they were crystallized appeared to have resulted in slightly different conformations for the cavity surrounding Asp52$^{2.50}$. In the two thermostabilized structures, the hydroxyl group side chains of Ser91$^{3.39}$ and Ser281$^{7.46}$ formed hydrogen bonds to Asp52$^{2.50}$. In addition, the backbone carbonyl of Asn284$^{7.49}$ was within hydrogen bonding distance of Asp52$^{2.50}$. As carbonyl groups can act as only hydrogen bond acceptors, this structure suggested that Asp52$^{2.50}$ was protonated (Figure 8B,C). However, it should be noted that one of the residues that has been mutated to stabilize the receptor for crystallization is part of the cavity surrounding Asp52$^{2.50}$ (L48A), which may affect the structure of the receptor in this region. In the third active-like structure (PDB entry 3QAK[8]), Pro285$^{7.50}$ moved into the cavity upon activation, which positions the backbone carbonyl of Ser281$^{7.46}$ (2.6 Å) within hydrogen bonding distance of the Asp52$^{2.50}$ carboxylate (Figure 8D). Interestingly, the resulting conformation of TM helix 7 and potential interaction with the backbone carbonyl of Ser281$^{7.46}$ were similar to certain snapshots from the MD simulation of the β_2AR with protonated Asp79$^{2.50}$ (Figure 7B). Protonation of Asp52$^{2.50}$ upon activation was also supported by calculations conducted with PROPKA,[57] which predicted pK_a values of 7.5 (ranging from 6.3 to 8) and 9.1 (ranging from 8.9 to 9.2) for the

dx.doi.org/10.1021/bi5008723 | Biochemistry 2014, 53, 7283−7296

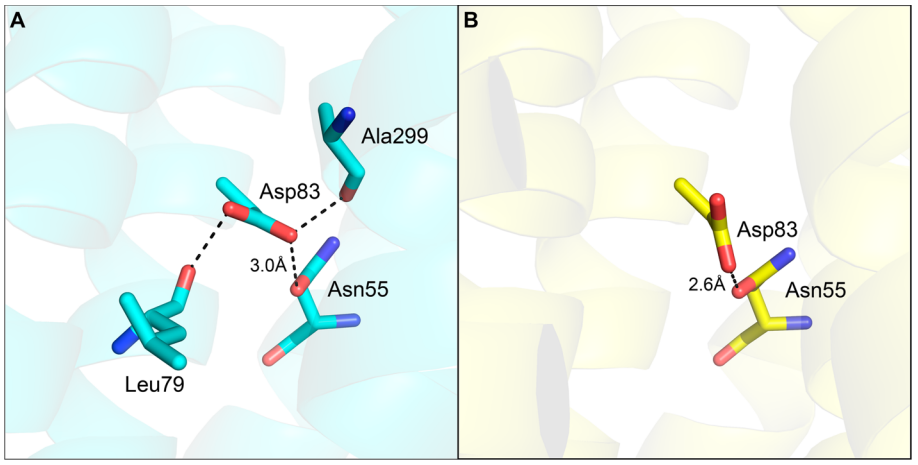

Figure 9. Analysis of the protonation state of Asp$^{2.50}$ in inactive- and active-like crystal structures of rhodopsin/opsin: (A) inactive-like (PDB entry IF88) and (B) active-like (PDB entry 3DQB). It should be noted that the side chain orientation of Asn55 has been rotated 180° to optimize the hydrogen bond network. Polar contacts within 3.2 Å of the carboxylate oxygens are shown as black dashed lines. The heavy atom distance (Å) is shown if the hydrogen bond is predicted to involve a protonated Asp$^{2.50}$ carboxylate. This figure was generated with PyMOL (version 1.4.1).

inactive- and active-like structures of the A_{2A}AR, respectively (Table S3 of the Supporting Information). In this case, the difference in pK_a between the two states appeared to originate from a direct interaction, e.g., with the backbone carbonyl of Asn284$^{7.49}$. In summary, the analysis of A_{2A}AR structures suggested both a reduction in the size of the cavity surrounding Asp52$^{2.50}$ and a shift in protonation upon activation.

In the case of rhodopsin/opsin, the large hydrated cavity observed in the inactive conformation was also collapsed in the active-like opsin structure (Figure 9A,B). In our analysis of three active-like rhodopsin/opsin structures (PDB entries 3DQB,[7] 3PQR, and 3PXO), we determined that the side chain orientation of Asn55$^{1.50}$ must be flipped 180° to satisfy a hydrogen bond interaction with the backbone carbonyl of Ala299$^{7.46}$, which can act as only a hydrogen bond acceptor. This was supported by visual inspection of the hydrogen bonding network as well as the structure validation tool Molprobity.[83] The resulting hydrogen bond network suggested that the side chain carboxylate of Asp83$^{2.50}$ was protonated in both states. The side chain carbonyl of Asn55$^{1.50}$ interacted with Asp83$^{2.50}$ in both the inactive and active rhodopsin structures (PDB entries 1F88 and 3DQB, respectively),[62] which supported protonated active and inactive states of this receptor. The two serine residues in the cavity that are conserved for both the A_{2A}AR and β_2AR are alanines in the case of rhodopsin (Ala124$^{3.39}$ and Ala299$^{7.46}$, respectively), which could also be expected to further increase the pK_a due to the loss of hydrogen bonding. As expected, the loss of these direct interactions led to elevated PROPKA pK_a values, which were equal to 9.2 for both the inactive and active-like structures (Table S3 of the Supporting Information).

DISCUSSION

The goal of this study was to understand the pH dependence of β_2AR activation[37] and to investigate if further understanding of the molecular origins of this effect could provide new insights into GPCR signaling. Access to both active and inactive conformations of the β_2AR allowed us to use MD simulations to explore the roles of Asp79$^{2.50}$ protonation in receptor activation at the atomic level, which are difficult to investigate from static crystal structures.

The burial of ionizable Asp79$^{2.50}$ in the transmembrane region and the structural changes observed in its immediate neighborhood upon activation point to a potential role for this residue in GPCR function. On the basis of the high degree of sequence conservation for Asp$^{2.50}$ among class A GPCRs, this residue has received considerable attention in previous studies of receptor function.[40−44] In early work, Strader et al. suggested that Asp79$^{2.50}$ was either directly involved in agonist binding or responsible for maintaining the active conformation.[41] More recently, Vanni et al. proposed that the ionized Asp79$^{2.50}$ favored activation based on up to 800 ns simulations of inactive state crystal structures.[20] However, these results could not explain the observed pH dependence of β_2AR activation. In our work, we took advantage of access to both active and inactive state crystal structures, which allowed us to probe the protonation state of Asp79$^{2.50}$ in both relevant conformations of the β_2AR. In contrast to the results of Vanni et al., our free energy simulations instead suggested that the protonated state of Asp79$^{2.50}$ was favored in the active conformation, a result that could explain the experimental observation that basal activity for the β_2AR is higher at pH 6.5 than at 8.0. Our MD simulations demonstrated that an ionized Asp79$^{2.50}$ is compatible with only an inactive-like conformation of the cavity surrounding this residue. This is further supported by the fact that a sodium ion has recently been identified in the vicinity of Asp$^{2.50}$ in several (inactive state) crystal structures of GPCRs[80] and, in addition, was observed in the same cavity in our analyzed simulation trajectories. The MD free energy calculations suggested that the shift in protonation state upon activation was primarily due to a loss of solvent interactions. In previous analyses of GPCR crystal structures, it has been suggested that conserved clusters of water molecules in the vicinity of Asp79$^{2.50}$ were important for receptor activation by bridging interactions between conserved residues.[33,34,84] Our simulations indicate that an additional role of these water clusters may be to regulate activation by modulating the ionization state of Asp79$^{2.50}$ and, possibly, by influencing the presence of sodium ions in the transmembrane cavity.

Long time scale simulations by Dror et al. allowed us to analyze the role of Asp79$^{2.50}$ in GPCR activation based on multiple MD trajectories initiated from an active state crystal structure of the β_2AR. Although simulations of ionized and

dx.doi.org/10.1021/bi5008723 | Biochemistry 2014, 53, 7283−7296

protonated trajectories of Asp79$^{2.50}$ were both found to reach inactive-like conformations, there were significant differences between these two simulation sets.[19] Our observations provide new interpretations of results from NMR experiments in which ^{13}C-labeled methionine residues of the β_2AR were monitored under different conditions.[13,14] Interestingly, several NMR peaks, indicating a number of different receptor conformations around Met82$^{2.53}$, were observed for the apo, antagonist-bound, and inverse agonist-bound states of the β_2AR. As Met82$^{2.53}$ is part of the cavity surrounding Asp79$^{2.50}$, we propose that these may reflect receptor conformations corresponding to the protonated and ionized forms of Asp79$^{2.50}$. This is consistent with a predicted pK_a of Asp79$^{2.50}$ close to physiological pH and the fact that microsecond MD simulations resulted in different volumes of the transmembrane cavity depending on the protonation state of this residue. This suggests an equilibrium, in which the cavity surrounding Asp79$^{2.50}$ could shrink and grow depending on the protonation state and result in distinct chemical environments around Met82$^{2.53}$. In the active and agonist-bound state of the β_2AR, the number of NMR peaks for Met82$^{2.53}$ was reduced to one, which suggested similar receptor conformations in this region under these two conditions.[14] This was surprising because crystal structures of the agonist-bound β_2AR in the absence of G-protein or nanobody have been very similar to inactive state conformations.[85] The difference between these results suggests that the relative population of different conformational states may be sensitive to the experimental conditions. We propose that the single peak observed in the NMR experiments for agonist-bound and active states may represent conditions in which Asp79$^{2.50}$ is protonated, which in our simulations correlated with a consistently smaller (more active-like) cavity volume. Together, these results could point to a potential role of Asp79$^{2.50}$ as a "protonation switch" that may be part of the complex network that connects the orthosteric site to intracellular G-protein coupling. This hypothesis is supported by the pH dependence of β_2AR activation. However, more experimental work is necessary to elucidate if agonist binding alone can influence the protonation state of Asp79$^{2.50}$ as there is currently no direct evidence of such a mechanism. Indeed, it is also possible that Asp79$^{2.50}$ protonation is a consequence of the conformational changes involved in activation, rather than part of the mechanism that transmits the signal across the membrane. In this context, it should also be noted that the conformations observed in our MD simulations and the transitions between them may be influenced by limitations associated with force field accuracy, lipid composition, system size, and simulation length.

The importance of Asp79$^{2.50}$ for GPCR activation is also supported by mutagenesis studies. Interestingly, Asp79$^{2.50}$Ala and Asp79$^{2.50}$Asn mutants bind antagonists with affinities similar to those of wild-type β_2AR, whereas the affinity for agonists is significantly reduced. The substitution of an ionizable Asp79 with Asn or Ala is also accompanied by a loss of G-protein signaling,[41,44] which could be interpreted as a neutral side chain favoring the inactive state. However, the equivalent Asp$^{2.50}$Ala mutation results in constitutive activity for the closely related β_1AR, suggesting that interpretation of mutagenesis in this region is complex.[86] The common assumption that asparagine is a good mimic of a protonated aspartic acid is also questionable. The polarities of side chain analogues of Asn and (protonated) Asp are quite different, as reflected by the 3 kcal/mol difference in hydration free energy for (neutral) acetic acid and acetamide.[87] What these observations do support is that Asp79$^{2.50}$ is critical for maintaining the balance between the active and inactive states.[41] The cavity surrounding Asp79$^{2.50}$ is composed of many highly conserved residues, which points to a regulatory role in activation. Basal activity has been shown to increase if Ser319$^{7.46}$, which can form hydrogen bonds to Asp79$^{2.50}$, is mutated to alanine.[88] Interestingly, sequence alignment of class A GPCRs has shown that the Ser319$^{7.46}$ position is typically occupied by small hydrophilic and hydrophobic residues such as Ser (63%), Cys (12%), Ala (7%), and Thr (6%).[39] Such differences may affect the pK_a of Asp79$^{2.50}$, which in turn could influence sodium- and receptor-dependent signaling properties such as basal activity. This analysis led us to the question of whether the proposed role of Asp$^{2.50}$ as a "protonation switch" can be transferred to other class A GPCRs. The structural conservation of the cavity surrounding Asp$^{2.50}$ in all crystal structures of class A receptors further strengthens the hypothesis that this region is important for receptor function. Our analysis of A_{2A}AR crystal structures of active- and inactive-like conformations, which share a high degree of sequence similarity with the β_2AR in this region, supported the idea that Asp$^{2.50}$ similarly undergoes a change in protonation state upon activation of this receptor. In addition, the conformation of TM helix 7 observed in certain simulations of the β_2AR conducted with the protonated Asp79$^{2.50}$ is strikingly similar to that observed in a crystal structure of the agonist-bound A_{2A}AR. This alternative TM7 conformation may thus be relevant for several GPCRs. On the other hand, crystal structures of rhodopsin/opsin structures instead suggested that Asp$^{2.50}$ is protonated in both states, which is in agreement with experimental data.[89] Taken together, these observations suggest that the role of Asp$^{2.50}$ as a "protonation switch" likely can be transferred to other, but not all, class A GPCRs.

In summary, the main result of this work is that the pH-dependent behavior of the β_2AR is primarily due to the buried and highly conserved Asp79$^{2.50}$. We propose that this residue has an elevated pK_a close to physiological pH and that a shift in protonation state for this residue may have a role as one of the microswitches for β_2AR activation. An improved molecular-level understanding of how the ionization state of the conserved Asp$^{2.50}$ influences the conformational equilibrium of the β_2AR will be important for understanding the complex process of GPCR activation.

■ ASSOCIATED CONTENT

Supporting Information

Supporting Figures S1−S9 and Tables S1−S3. This material is available free of charge via the Internet at http://pubs.acs.org.

■ AUTHOR INFORMATION

Corresponding Author

*Science for Life Laboratory, Box 1031, SE-171 21 Solna, Sweden, or Department of Biochemistry and Biophysics and Center for Biomembrane Research, Stockholm University, SE-106 91 Stockholm, Sweden. E-mail: jens.carlsson@dbb.su.se.

Funding

This work was supported by grants from the Knut and Alice Wallenberg foundation and the Swedish Foundation for Strategic Research to J.C.

Notes

The authors declare no competing financial interest.

■ ACKNOWLEDGMENTS

Computational resources were provided by the Swedish National Infrastructure for Computing (SNIC) and the National Supercomputer Centre (NSC) in Linköping, Sweden. We thank D.E. Shaw Research for providing access to MD simulation trajectories of the β_2AR.

■ ABBREVIATIONS

MD, molecular dynamics; GPCR, G-protein-coupled receptor; TM, transmembrane; ICL, intracellular loop; β_2AR, β_2 adrenergic receptor; β_1AR, β_1 adrenergic receptor; A_{2A}AR, A_{2A} adenosine receptor; M_2MR, M2 muscarinic receptor; PAR-1, protease-activated receptor type 1; δ-OR, δ-opioid receptor; FEP, free energy perturbation; rmsd, root-mean-square deviation.

■ REFERENCES

(1) Lagerstrom, M. C., and Schioth, H. B. (2008) Structural diversity of G protein-coupled receptors and significance for drug discovery. *Nat. Rev. Drug Discovery 7*, 339−357.

(2) Katritch, V., Cherezov, V., and Stevens, R. C. (2013) Structure-function of the G protein-coupled receptor superfamily. *Annu. Rev. Pharmacol. Toxicol. 53*, 531−556.

(3) Cherezov, V., Rosenbaum, D. M., Hanson, M. A., Rasmussen, S. G., Thian, F. S., Kobilka, T. S., Choi, H. J., Kuhn, P., Weis, W. I., Kobilka, B. K., and Stevens, R. C. (2007) High-resolution crystal structure of an engineered human β2-adrenergic G protein-coupled receptor. *Science 318*, 1258−1265.

(4) Rasmussen, S. G., DeVree, B. T., Zou, Y., Kruse, A. C., Chung, K. Y., Kobilka, T. S., Thian, F. S., Chae, P. S., Pardon, E., Calinski, D., Mathiesen, J. M., Shah, S. T., Lyons, J. A., Caffrey, M., Gellman, S. H., Steyaert, J., Skiniotis, G., Weis, W. I., Sunahara, R. K., and Kobilka, B. K. (2011) Crystal structure of the β2 adrenergic receptor-Gs protein complex. *Nature 477*, 549−555.

(5) Chung, K. Y., Rasmussen, S. G., Liu, T., Li, S., DeVree, B. T., Chae, P. S., Calinski, D., Kobilka, B. K., Woods, V. L., Jr., and Sunahara, R. K. (2011) Conformational changes in the G protein Gs induced by the β2 adrenergic receptor. *Nature 477*, 611−615.

(6) Park, J. H., Scheerer, P., Hofmann, K. P., Choe, H. W., and Ernst, O. P. (2008) Crystal structure of the ligand-free G-protein-coupled receptor opsin. *Nature 454*, 183−187.

(7) Scheerer, P., Park, J. H., Hildebrand, P. W., Kim, Y. J., Krauss, N., Choe, H. W., Hofmann, K. P., and Ernst, O. P. (2008) Crystal structure of opsin in its G-protein-interacting conformation. *Nature 455*, 497−502.

(8) Xu, F., Wu, H., Katritch, V., Han, G. W., Jacobson, K. A., Gao, Z. G., Cherezov, V., and Stevens, R. C. (2011) Structure of an agonist-bound human A2A adenosine receptor. *Science 332*, 322−327.

(9) Lebon, G., Warne, T., Edwards, P. C., Bennett, K., Langmead, C. J., Leslie, A. G., and Tate, C. G. (2011) Agonist-bound adenosine A2A receptor structures reveal common features of GPCR activation. *Nature 474*, 521−525.

(10) Kruse, A. C., Ring, A. M., Manglik, A., Hu, J. X., Hu, K., Eitel, K., Hubner, H., Pardon, E., Valant, C., Sexton, P. M., Christopoulos, A., Felder, C. C., Gmeiner, P., Steyaert, J., Weis, W. I., Garcia, K. C., Wess, J., and Kobilka, B. K. (2013) Activation and allosteric modulation of a muscarinic acetylcholine receptor. *Nature 504*, 101−106.

(11) Haga, K., Kruse, A. C., Asada, H., Yurugi-Kobayashi, T., Shiroishi, M., Zhang, C., Weis, W. I., Okada, T., Kobilka, B. K., Haga, T., and Kobayashi, T. (2012) Structure of the human M2 muscarinic acetylcholine receptor bound to an antagonist. *Nature 482*, 547−551.

(12) Kobilka, B. K., and Deupi, X. (2007) Conformational complexity of G-protein-coupled receptors. *Trends Pharmacol. Sci. 28*, 397−406.

(13) Kofuku, Y., Ueda, T., Okude, J., Shiraishi, Y., Kondo, K., Maeda, M., Tsujishita, H., and Shimada, I. (2012) Efficacy of the β_2-adrenergic receptor is determined by conformational equilibrium in the transmembrane region. *Nat. Commun. 3*, 1045.

(14) Nygaard, R., Zou, Y., Dror, R. O., Mildorf, T. J., Arlow, D. H., Manglik, A., Pan, A. C., Liu, C. W., Fung, J. J., Bokoch, M. P., Thian, F. S., Kobilka, T. S., Shaw, D. E., Mueller, L., Prosser, R. S., and Kobilka, B. K. (2013) The dynamic process of β_2-adrenergic receptor activation. *Cell 152*, 532−542.

(15) Liu, J. J., Horst, R., Katritch, V., Stevens, R. C., and Wuthrich, K. (2012) Biased signaling pathways in β2-adrenergic receptor characterized by ^{19}F-NMR. *Science 335*, 1106−1110.

(16) Yao, X., Parnot, C., Deupi, X., Ratnala, V. R., Swaminath, G., Farrens, D., and Kobilka, B. (2006) Coupling ligand structure to specific conformational switches in the β2-adrenoceptor. *Nat. Chem. Biol. 2*, 417−422.

(17) Rasmussen, S. G., Choi, H. J., Fung, J. J., Pardon, E., Casarosa, P., Chae, P. S., Devree, B. T., Rosenbaum, D. M., Thian, F. S., Kobilka, T. S., Schnapp, A., Konetzki, I., Sunahara, R. K., Gellman, S. H., Pautsch, A., Steyaert, J., Weis, W. I., and Kobilka, B. K. (2011) Structure of a nanobody-stabilized active state of the β_2 adrenoceptor. *Nature 469*, 175−180.

(18) Dror, R. O., Arlow, D. H., Borhani, D. W., Jensen, M. O., Piana, S., and Shaw, D. E. (2009) Identification of two distinct inactive conformations of the β2-adrenergic receptor reconciles structural and biochemical observations. *Proc. Natl. Acad. Sci. U.S.A. 106*, 4689−4694.

(19) Dror, R. O., Arlow, D. H., Maragakis, P., Mildorf, T. J., Pan, A. C., Xu, H., Borhani, D. W., and Shaw, D. E. (2011) Activation mechanism of the β2-adrenergic receptor. *Proc. Natl. Acad. Sci. U.S.A. 108*, 18684−18689.

(20) Vanni, S., Neri, M., Tavernelli, I., and Rothlisberger, U. (2010) A conserved protonation-induced switch can trigger "ionic-lock" formation in adrenergic receptors. *J. Mol. Biol. 397*, 1339−1349.

(21) Bhattacharya, S., and Vaidehi, N. (2010) Computational mapping of the conformational transitions in agonist selective pathways of a G-protein coupled receptor. *J. Am. Chem. Soc. 132*, 5205−5214.

(22) Nygaard, R., Frimurer, T. M., Holst, B., Rosenkilde, M. M., and Schwartz, T. W. (2009) Ligand binding and micro-switches in 7TM receptor structures. *Trends Pharmacol. Sci. 30*, 249−259.

(23) Ballesteros, J. A., Jensen, A. D., Liapakis, G., Rasmussen, S. G., Shi, L., Gether, U., and Javitch, J. A. (2001) Activation of the β2-adrenergic receptor involves disruption of an ionic lock between the cytoplasmic ends of transmembrane segments 3 and 6. *J. Biol. Chem. 276*, 29171−29177.

(24) Shi, L., Liapakis, G., Xu, R., Guarnieri, F., Ballesteros, J. A., and Javitch, J. A. (2002) β2 adrenergic receptor activation. Modulation of the proline kink in transmembrane 6 by a rotamer toggle switch. *J. Biol. Chem. 277*, 40989−40996.

(25) Ballesteros, J. A., and Weinstein, H. (1995) Integrated methods for the construction of three-dimensional models of structure−function relations in G protein-coupled receptors. *Methods Neurosci. 25*, 366−428.

(26) Moukhametzianov, R., Warne, T., Edwards, P. C., Serrano-Vega, M. J., Leslie, A. G., Tate, C. G., and Schertler, G. F. (2011) Two distinct conformations of helix 6 observed in antagonist-bound structures of a β1-adrenergic receptor. *Proc. Natl. Acad. Sci. U.S.A. 108*, 8228−8232.

(27) Hanson, M. A., Cherezov, V., Griffith, M. T., Roth, C. B., Jaakola, V. P., Chien, E. Y., Velasquez, J., Kuhn, P., and Stevens, R. C. (2008) A specific cholesterol binding site is established by the 2.8 Å structure of the human β2-adrenergic receptor. *Structure 16*, 897−905.

(28) Liu, W., Chun, E., Thompson, A. A., Chubukov, P., Xu, F., Katritch, V., Han, G. W., Roth, C. B., Heitman, L. H., IJzerman, A. P., Cherezov, V., and Stevens, R. C. (2012) Structural basis for allosteric regulation of GPCRs by sodium ions. *Science 337*, 232−236.

(29) Zocher, M., Fung, J. J., Kobilka, B. K., and Muller, D. J. (2012) Ligand-specific interactions modulate kinetic, energetic, and mechanical properties of the human β2 adrenergic receptor. *Structure 20*, 1391−1402.

(30) Gutierrez-de-Teran, H., Massink, A., Rodriguez, D., Liu, W., Han, G. W., Joseph, J. S., Katritch, I., Heitman, L. H., Xia, L., Ijzerman, A. P., Cherezov, V., Katritch, V., and Stevens, R. C. (2013) The role of a sodium ion binding site in the allosteric modulation of the A(2A) adenosine G protein-coupled receptor. *Structure 21*, 2175−2185.
(31) Zhang, C., Srinivasan, Y., Arlow, D. H., Fung, J. J., Palmer, D., Zheng, Y., Green, H. F., Pandey, A., Dror, R. O., Shaw, D. E., Weis, W. I., Coughlin, S. R., and Kobilka, B. K. (2012) High-resolution crystal structure of human protease-activated receptor 1. *Nature 492*, 387−392.
(32) Miller-Gallacher, J. L., Nehmé, R., Warne, T., Edwards, P. C., Schertler, G. F. X., Leslie, A. G. W., and Tate, C. G. (2014) The 2.1 Å Resolution Structure of Cyanopindolol-Bound β1 Adrenoceptor Identifies an Intramembrane Na^+ Ion that Stabilises the Ligand-Free Receptor. *PLoS One 9*, e92727.
(33) Angel, T. E., Chance, M. R., and Palczewski, K. (2009) Conserved waters mediate structural and functional activation of family A (rhodopsin-like) G protein-coupled receptors. *Proc. Natl. Acad. Sci. U.S.A. 106*, 8555−8560.
(34) Pardo, L., Deupi, X., Dolker, N., Lopez-Rodriguez, M. L., and Campillo, M. (2007) The role of internal water molecules in the structure and function of the rhodopsin family of G protein-coupled receptors. *ChemBioChem 8*, 19−24.
(35) Nygaard, R., Valentin-Hansen, L., Mokrosinski, J., Frimurer, T. M., and Schwartz, T. W. (2010) Conserved water-mediated hydrogen bond network between TM-I, -II, -VI, and -VII in 7TM receptor activation. *J. Biol. Chem. 285*, 19625−19636.
(36) Neve, K. A. (1991) Regulation of dopamine D2 receptors by sodium and pH. *Mol. Pharmacol. 39*, 570−578.
(37) Ghanouni, P., Schambye, H., Seifert, R., Lee, T. W., Rasmussen, S. G., Gether, U., and Kobilka, B. K. (2000) The effect of pH on β_2 adrenoceptor function. Evidence for protonation-dependent activation. *J. Biol. Chem. 275*, 3121−3127.
(38) Arnis, S., Fahmy, K., Hofmann, K. P., and Sakmar, T. P. (1994) A conserved carboxylic acid group mediates light-dependent proton uptake and signaling by rhodopsin. *J. Biol. Chem. 269*, 23879−23881.
(39) Mirzadegan, T., Benko, G., Filipek, S., and Palczewski, K. (2003) Sequence analyses of G-protein-coupled receptors: Similarities to rhodopsin. *Biochemistry 42*, 2759−2767.
(40) Proulx, C. D., Holleran, B. J., Boucard, A. A., Escher, E., Guillemette, G., and Leduc, R. (2008) Mutational analysis of the conserved Asp2.50 and ERY motif reveals signaling bias of the urotensin II receptor. *Mol. Pharmacol. 74*, 552−561.
(41) Strader, C. D., Sigal, I. S., Candelore, M. R., Rands, E., Hill, W. S., and Dixon, R. A. (1988) Conserved aspartic acid residues 79 and 113 of the β-adrenergic receptor have different roles in receptor function. *J. Biol. Chem. 263*, 10267−10271.
(42) Parker, M. S., Wong, Y. Y., and Parker, S. L. (2008) An ion-responsive motif in the second transmembrane segment of rhodopsin-like receptors. *Amino Acids 35*, 1−15.
(43) Bihoreau, C., Monnot, C., Davies, E., Teutsch, B., Bernstein, K. E., Corvol, P., and Clauser, E. (1993) Mutation of Asp74 of the rat angiotensin II receptor confers changes in antagonist affinities and abolishes G-protein coupling. *Proc. Natl. Acad. Sci. U.S.A. 90*, 5133−5137.
(44) Chung, F. Z., Wang, C. D., Potter, P. C., Venter, J. C., and Fraser, C. M. (1988) Site-Directed Mutagenesis and Continuous Expression of Human β-Adrenergic Receptors: Identification of a Conserved Aspartate Residue Involved in Agonist Binding and Receptor Activation. *J. Biol. Chem. 263*, 4052−4055.
(45) Hess, B., Kutzner, C., van der Spoel, D., and Lindahl, E. (2008) GROMACS 4: Algorithms for highly efficient, load-balanced, and scalable molecular simulation. *J. Chem. Theory Comput. 4*, 435−447.
(46) Jorgensen, W. L., Maxwell, D. S., and TiradoRives, J. (1996) Development and testing of the OPLS all-atom force field on conformational energetics and properties of organic liquids. *J. Am. Chem. Soc. 118*, 11225−11236.
(47) Jorgensen, W. L., Chandrasekhar, J., Madura, J. D., Impey, R. W., and Klein, M. L. (1983) Comparison of Simple Potential Functions for Simulating Liquid Water. *J. Chem. Phys. 79*, 926−935.
(48) Berger, O., Edholm, O., and Jahnig, F. (1997) Molecular dynamics simulations of a fluid bilayer of dipalmitoylphosphatidylcholine at full hydration, constant pressure, and constant temperature. *Biophys. J. 72*, 2002−2013.
(49) Marelius, J., Kolmodin, K., Feierberg, I., and Aqvist, J. (1998) Q: A molecular dynamics program for free energy calculations and empirical valence bond simulations in biomolecular systems. *J. Mol. Graphics Modell. 16*, 213−225.
(50) Berendsen, H. J. C., Postma, J. P. M., Vangunsteren, W. F., Dinola, A., and Haak, J. R. (1984) Molecular-Dynamics with Coupling to an External Bath. *J. Chem. Phys. 81*, 3684−3690.
(51) Aqvist, J. (1996) Calculation of absolute binding free energies for charged ligands and effects of long-range electrostatic interactions. *J. Comput. Chem. 17*, 1587−1597.
(52) Ryckaert, J. P., Ciccotti, G., and Berendsen, H. J. C. (1977) Numerical-Integration of Cartesian Equations of Motion of a System with Constraints: Molecular-Dynamics of N-Alkanes. *J. Comput. Phys. 23*, 327−341.
(53) King, G., and Warshel, A. (1989) A Surface Constrained All-Atom Solvent Model for Effective Simulations of Polar Solutions. *J. Chem. Phys. 91*, 3647−3661.
(54) Lee, F. S., and Warshel, A. (1992) A Local Reaction Field Method for Fast Evaluation of Long-Range Electrostatic Interactions in Molecular Simulations. *J. Chem. Phys. 97*, 3100−3107.
(55) Kollman, P. (1993) Free energy calculations: Applications to chemical and biochemical phenomena. *Chem. Rev. 93*, 2395−2417.
(56) Brandsdal, B. O., Smalas, A. O., and Aqvist, J. (2006) Free energy calculations show that acidic P1 variants undergo large pKa shifts upon binding to trypsin. *Proteins 64*, 740−748.
(57) Li, H., Robertson, A. D., and Jensen, J. H. (2005) Very fast empirical prediction and rationalization of protein pKa values. *Proteins 61*, 704−721.
(58) Wacker, D., Fenalti, G., Brown, M. A., Katritch, V., Abagyan, R., Cherezov, V., and Stevens, R. C. (2010) Conserved binding mode of human β2 adrenergic receptor inverse agonists and antagonist revealed by X-ray crystallography. *J. Am. Chem. Soc. 132*, 11443−11445.
(59) Ring, A. M., Manglik, A., Kruse, A. C., Enos, M. D., Weis, W. I., Garcia, K. C., and Kobilka, B. K. (2013) Adrenaline-activated structure of β-adrenoceptor stabilized by an engineered nanobody. *Nature 502*, 575−579.
(60) Li, J., Edwards, P. C., Burghammer, M., Villa, C., and Schertler, G. F. (2004) Structure of bovine rhodopsin in a trigonal crystal form. *J. Mol. Biol. 343*, 1409−1438.
(61) Okada, T., Sugihara, M., Bondar, A. N., Elstner, M., Entel, P., and Buss, V. (2004) The retinal conformation and its environment in rhodopsin in light of a new 2.2 Å crystal structure. *J. Mol. Biol. 342*, 571−583.
(62) Palczewski, K., Kumasaka, T., Hori, T., Behnke, C. A., Motoshima, H., Fox, B. A., Le Trong, I., Teller, D. C., Okada, T., Stenkamp, R. E., Yamamoto, M., and Miyano, M. (2000) Crystal structure of rhodopsin: A G protein-coupled receptor. *Science 289*, 739−745.
(63) Salom, D., Lodowski, D. T., Stenkamp, R. E., Le Trong, I., Golczak, M., Jastrzebska, B., Harris, T., Ballesteros, J. A., and Palczewski, K. (2006) Crystal structure of a photoactivated deprotonated intermediate of rhodopsin. *Proc. Natl. Acad. Sci. U.S.A. 103*, 16123−16128.
(64) Stenkamp, R. E. (2008) Alternative models for two crystal structures of bovine rhodopsin. *Acta Crystallogr. D64*, 902−904.
(65) Teller, D. C., Okada, T., Behnke, C. A., Palczewski, K., and Stenkamp, R. E. (2001) Advances in determination of a high-resolution three-dimensional structure of rhodopsin, a model of G-protein-coupled receptors (GPCRs). *Biochemistry 40*, 7761−7772.
(66) Congreve, M., Andrews, S. P., Dore, A. S., Hollenstein, K., Hurrell, E., Langmead, C. J., Mason, J. S., Ng, I. W., Tehan, B., Zhukov, A., Weir, M., and Marshall, F. H. (2012) Discovery of 1,2,4-Triazine

Derivatives as Adenosine A(2A) Antagonists using Structure Based Drug Design. *J. Med. Chem. 55*, 1898−1903.
(67) Dore, A. S., Robertson, N., Errey, J. C., Ng, I., Hollenstein, K., Tehan, B., Hurrell, E., Bennett, K., Congreve, M., Magnani, F., Tate, C. G., Weir, M., and Marshall, F. H. (2011) Structure of the Adenosine A(2A) Receptor in Complex with ZM241385 and the Xanthines XAC and Caffeine. *Structure 19*, 1283−1293.
(68) Jaakola, V. P., Griffith, M. T., Hanson, M. A., Cherezov, V., Chien, E. Y., Lane, J. R., Ijzerman, A. P., and Stevens, R. C. (2008) The 2.6 angstrom crystal structure of a human A2A adenosine receptor bound to an antagonist. *Science 322*, 1211−1217.
(69) Hoover, W. G. (1985) Canonical Dynamics: Equilibrium Phase-Space Distributions. *Phys. Rev. A 31*, 1695−1697.
(70) Nose, S. (1984) A Unified Formulation of the Constant Temperature Molecular-Dynamics Methods. *J. Chem. Phys. 81*, 511−519.
(71) Parrinello, M., and Rahman, A. (1981) Polymorphic Transitions in Single-Crystals: A New Molecular-Dynamics Method. *J. Appl. Phys. 52*, 7182−7190.
(72) Darden, T., York, D., and Pedersen, L. (1993) Particle Mesh Ewald: An N.Log(N) Method for Ewald Sums in Large Systems. *J. Chem. Phys. 98*, 10089−10092.
(73) Hess, B., Bekker, H., Berendsen, H. J. C., and Fraaije, J. G. E. M. (1997) LINCS: A linear constraint solver for molecular simulations. *J. Comput. Chem. 18*, 1463−1472.
(74) Schmidtke, P., Le Guilloux, V., Maupetit, J., and Tuffery, P. (2010) fpocket: Online tools for protein ensemble pocket detection and tracking. *Nucleic Acids Res. 38*, W582−W589.
(75) Elcock, A. H. (2001) Prediction of functionally important residues based solely on the computed energetics of protein structure. *J. Mol. Biol. 312*, 885−896.
(76) Simonson, T., Carlsson, J., and Case, D. A. (2004) Proton binding to proteins: pK_a calculations with explicit and implicit solvent models. *J. Am. Chem. Soc. 126*, 4167−4180.
(77) Warshel, A., Sussman, F., and King, G. (1986) Free energy of charges in solvated proteins: Microscopic calculations using a reversible charging process. *Biochemistry 25*, 8368−8372.
(78) Davies, M. N., Toseland, C. P., Moss, D. S., and Flower, D. R. (2006) Benchmarking pK_a prediction. *BMC Biochem. 7*, 18.
(79) Olsson, M. H. M., Sondergaard, C. R., Rostkowski, M., and Jensen, J. H. (2011) PROPKA3: Consistent Treatment of Internal and Surface Residues in Empirical pK_a Predictions. *J. Chem. Theory Comput. 7*, 525−537.
(80) Katritch, V., Fenalti, G., Abola, E. E., Roth, B. L., Cherezov, V., and Stevens, R. C. (2014) Allosteric sodium in class A GPCR signaling. *Trends Biochem. Sci. 39*, 233−244.
(81) Seifert, R. (2001) Monovalent anions differentially modulate coupling of the β2-adrenoceptor to G(s)α splice variants. *J. Pharmacol. Exp. Ther. 298*, 840−847.
(82) Hino, T., Arakawa, T., Iwanari, H., Yurugi-Kobayashi, T., Ikeda-Suno, C., Nakada-Nakura, Y., Kusano-Arai, O., Weyand, S., Shimamura, T., Nomura, N., Cameron, A. D., Kobayashi, T., Hamakubo, T., Iwata, S., and Murata, T. (2012) G-protein-coupled receptor inactivation by an allosteric inverse-agonist antibody. *Nature 482*, 237−240.
(83) Davis, I. W., Leaver-Fay, A., Chen, V. B., Block, J. N., Kapral, G. J., Wang, X., Murray, L. W., Arendall, W. B., Snoeyink, J., Richardson, J. S., and Richardson, D. C. (2007) MolProbity: All-atom contacts and structure validation for proteins and nucleic acids. *Nucleic Acids Res. 35*, W375−W383.
(84) Sugihara, M., Fujibuchi, W., and Suwa, M. (2011) Structural elements of the signal propagation pathway in squid rhodopsin and bovine rhodopsin. *J. Phys. Chem. B 115*, 6172−6179.
(85) Rosenbaum, D. M., Zhang, C., Lyons, J. A., Holl, R., Aragao, D., Arlow, D. H., Rasmussen, S. G., Choi, H. J., Devree, B. T., Sunahara, R. K., Chae, P. S., Gellman, S. H., Dror, R. O., Shaw, D. E., Weis, W. I., Caffrey, M., Gmeiner, P., and Kobilka, B. K. (2011) Structure and function of an irreversible agonist-β(2) adrenoceptor complex. *Nature 469*, 236−240.
(86) Ahmed, M., Muntasir, H. A., Hossain, M., Ishiguro, M., Komiyama, T., Muramatsu, I., Kurose, H., and Nagatomo, T. (2006) β-blockers show inverse agonism to a novel constitutively active mutant of β1-adrenoceptor. *J. Pharmacol. Sci. 102*, 167−172.
(87) Cabani, S., Gianni, P., Mollica, V., and Lepori, L. (1981) Group contributions to the thermodynamic properties of non-ionic organic solutes in dilute aqueous solution. *J. Solution Chem. 10*, 563−595.
(88) Arakawa, M., Chakraborty, R., Upadhyaya, J., Eilers, M., Reeves, P. J., Smith, S. O., and Chelikani, P. (2011) Structural and functional roles of small group-conserved amino acids present on helix-H7 in the β(2)-adrenergic receptor. *Biochim. Biophys. Acta 1808*, 1170−1178.
(89) Fahmy, K., Jager, F., Beck, M., Zvyaga, T. A., Sakmar, T. P., and Siebert, F. (1993) Protonation states of membrane-embedded carboxylic acid groups in rhodopsin and metarhodopsin II: A Fourier-transform infrared spectroscopy study of site-directed mutants. *Proc. Natl. Acad. Sci. U.S.A. 90*, 10206−10210.